

# Catchment-scale Phosphorus Export through Surface and Drainage Pathways

Conrad E. Brendel, Michelle L. Soupir,\* Leigh Ann M. Long, Matthew J. Helmers, Charles D. Ikenberry, and Amy L. Kaleita

## Abstract

The site-specific nature of P fate and transport in drained areas exemplifies the need for additional data to guide implementation of conservation practices at the catchment scale. Total P (TP), dissolved reactive P (DRP), and total suspended solids (TSS) were monitored at five sites—two streams, two tile outlets, and a grassed waterway—in three agricultural subwatersheds (221.2–822.5 ha) draining to Black Hawk Lake in western Iowa. Median TP concentrations ranged from 0.034 to 1.490 and 0.008 to 0.055 mg P L<sup>-1</sup> for event and baseflow samples, respectively. The majority of P and TSS export occurred during precipitation events and high-flow conditions with greater than 75% of DRP, 66% of TP, and 59% of TSS export occurring during the top 25% of flows from all sites. In one subwatershed, a single event (annual recurrence interval < 1 yr) was responsible for 46.6, 84.0, and 81.0% of the annual export of TP, DRP, and TSS, respectively, indicating that frequent, small storms have the potential to result in extreme losses. Isolated monitoring of surface and drainage transport pathways indicated significant P and TSS losses occurring through drainage; over the 2-yr study period, the drainage pathway was responsible for 69.8, 59.2, and 82.6% of the cumulative TP, DRP, and TSS export, respectively. Finally, the results provided evidence that particulate P losses in drainage were greater than dissolved P losses. Understanding relationships between flow, precipitation, transport pathway, and P fraction at the catchment scale is needed for effective conservation practice implementation.

## Core Ideas

- Single events accounted for the vast majority of annual P and total suspended solids export.
- Frequent, low-depth events resulted in extreme P and total suspended solids losses.
- Particulate P losses in drainage waters can exceed dissolved P losses.

**E**UTROPHICATION is a global issue affecting water bodies around the world, including North America's Gulf of Mexico, Northern Europe's Baltic Sea, and China's Changjiang estuary (Howarth and Paerl, 2008; Kleinman et al., 2011). Historically, productivity in coastal waters is limited by N, whereas P is the priority nutrient limiting upstream freshwater productivity (Paerl, 2009). Of human-induced imbalances, agricultural activities such as fertilizer and manure application are consistently identified as significant sources of P to surface waters (Torrent et al., 2007; Turner et al., 2007; Blann et al., 2009; Kronvang et al., 2009). For example, in the Gulf of Mexico, model simulations have indicated agriculture is responsible for >70% of the P input (Alexander et al., 2008). Within agricultural landscapes, subsurface drainage is an important pathway of P loading to the Mississippi River basin (Algoazany et al., 2007; Gentry et al., 2007; Tomer et al., 2010; King et al., 2015), Lake Erie (Culley et al., 1983; Tan and Zhang, 2011; Sharpley and Wang, 2014; Smith et al., 2015), the Chesapeake Bay (Keppler and Rhoderick, 2015), and the Baltic Sea (Behrendt and Bachor, 1998).

Artificial subsurface drainage is crucial to the success of row-crop agriculture in the Upper Midwestern United States. The use of drainage has transformed this region, previously covered in swamps and wetlands, into some of the world's most fertile agricultural land (Du et al., 2005). The benefits of subsurface drainage include allowing for trafficable conditions for timely field operations in seasonally and perennially wet locations, preventing excessive soil water conditions, providing salinity control in irrigated areas, and increasing nutrient uptake of crops by creating a well-aerated root environment (Reeve and Fausey, 1974; Fausey et al., 1987; Vos, 1987; Zucker and Brown, 1998; Du et al., 2005). Although drainage provides many benefits to agricultural production, drainage also represents a major pathway for nutrient losses from agricultural lands. Historically, studies of P export to waters have primarily focused on surface pathways, with some studies even suggesting that subsurface drainage reduces

Copyright © American Society of Agronomy, Crop Science Society of America, and Soil Science Society of America. 5585 Guilford Rd., Madison, WI 53711 USA. All rights reserved.

J. Environ. Qual. 48:117–126 (2019)  
doi:10.2134/jeq2018.07.0265

This is an open access article distributed under the terms of the CC BY-NC-ND license (<http://creativecommons.org/licenses/by-nc-nd/4.0/>).

Supplemental material is available online for this article.

Received 10 July 2018.

Accepted 25 Oct. 2018.

\*Corresponding author (msoupir@iastate.edu).

C.E. Brendel, M.L. Soupir, L.A.M. Long, M.J. Helmers, and A.L. Kaleita, Dep. of Agricultural & Biosystems Engineering, Iowa State Univ., Ames, IA 50011; C.E. Brendel, current address, Dep. of Civil & Environmental Engineering, Virginia Tech Univ., Blacksburg, VA 24061; C.D. Ikenberry, FYRA Engineering, Des Moines, IA 50309. Assigned to Associate Editor Heather Gall.

**Abbreviations:** ARI, annual recurrence interval; BFW, baseflow flow-weighted; BMP, best management practice; BHL, Black Hawk Lake; DRP, dissolved reactive phosphorus; EFW, event flow-weighted; OR, outflow ratio; S8, grassed waterway monitoring location in Subwatershed 8; S11, stream monitoring location in Subwatershed 11; S12, stream monitoring location in Subwatershed 12; T8, tile outlet monitoring location in Subwatershed 8; T12, tile outlet monitoring location in Subwatershed 12; TP, total phosphorus; TSS, total suspended solids; WY, water yield.

overall P export through reduced surface runoff (Bottcher et al., 1981; Bengtson et al., 1988; Fausey et al., 1995; Eastman et al., 2010). However, in shifting water flow from surface to subsurface pathways, substantial drainage P contributions have been reported, ranging from 17 to >50% of total P losses (Culley et al., 1983; Jamieson et al., 2003; Enright and Madramootoo, 2004; Tomer et al., 2010; King et al., 2015; Smith et al., 2015).

Phosphorus enters drainage through three primary pathways: (i) leaching into shallow groundwater through the soil matrix, (ii) preferential flow through macropores, and (iii) runoff to surface intakes diverted to tile lines. Soils with high P concentrations and low P sorption capacity have high potential for P to leach from the soil matrix into runoff and groundwater (Kleinman et al., 2007; Vadas et al., 2007). As soil moisture content decreases, the relative contribution of macropores to chemical transport and water movement increases (Shipitalo and Edwards, 1996). Geohring et al. (2001) studied the timing of drainage P transport relative to drainage flow and concluded that macropore flow is the primary transport pathway of total P (TP) through soil. Other studies have also highlighted the importance of the macropore pathway in P transport (Heathwaite and Dils, 2000; Simard et al., 2000; Vidon and Cuadra, 2011; Williams et al., 2016). When ponding occurs on the soil surface, P may also enter subsurface drainage through surface intakes. This pathway has been reported to deliver at least 75% of the drainage TP load (Tomer et al., 2010).

Although drainage is an important pathway influencing P export, there is a need for catchment-scale monitoring to provide comprehensive insight into the multiple factors and pathways influencing P losses from intensively drained agricultural watersheds. The specific objectives of this study were (i) to assess the impact of flow regime on P and total suspended solids (TSS) export; (ii) within event and baseflow conditions, to examine the partitioning of P into dissolved and sediment associated fractions; and (iii) to quantify analyte concentrations and loads in drainage and surface pathways. In watersheds with a complex mixture of small fields and landscape parcels, the water quality benefits of best management practice (BMP) implementation are most likely to be observed at the catchment scale (Stuart et al., 2010). Thus, this is the scale at which information is needed to inform optimized BMP implementation.

## Materials and Methods

### Study Area and Monitoring Sites

Three subwatersheds (8, 11, and 12) of Black Hawk Lake (BHL) in Carroll and Sac Counties, Iowa (Fig. 1), were monitored. The BHL watershed has a drainage area of 5324 ha and is located along the western edge of the Des Moines Lobe. This landform region is characterized by a gently rolling landscape with abundant moraines and prairie pothole wetlands, and silty clay loam soils formed in glacial till. Many of these potholes have been drained with underground tile lines to facilitate agriculture; row crops (corn [*Zea mays* L.] and soybeans [*Glycine max* (L.) Merr.]) account for 74.6% of the land use.

Subwatershed 8 (822.5 ha) is the largest of the three monitored subwatersheds. A 91-cm-diam. drainage district tile discharges just upstream of the subwatershed outlet. A second 30.5-cm tile also discharged at the same location but could not

be monitored because it was submerged during the study period. Samples were collected from the tile outlet (T8) and a grassed waterway (S8) that discharges at the same location. A 4.91-m-wide, 0.18-m-tall wooden weir was constructed at the grassed waterway discharge location to aid in sample collection and flow monitoring. Although sites T8 and S8 are located slightly upstream of the subwatershed outlet, elevated berms along the channel between the monitoring sites and the subwatershed outlet prevent runoff from entering the channel. Thus, the two monitoring sites are accurate representations of the total surface and drainage outflows from the subwatershed.

Subwatershed 11 is 229.4 ha; surface flow samples were collected from the middle of a concrete box culvert (S11). Flow through the culvert occurs nearly year-round, which suggests the presence of an upstream artificial drainage source in addition to runoff flow. Subwatershed 12 (221.2 ha) is similar in size to Subwatershed 11. Sample collection occurred on both sides of a concrete box culvert; surface flow samples were collected upstream of the culvert at a 1.83-m-wide, 17.8-cm-tall wooden weir (S12), and drainage flow samples were collected from a 39.4-cm-diam. tile located downstream of the culvert (T12). Flow at S12 is fed by runoff as well as upstream artificial drainage sources, including a 25.4-cm-diam. tile outlet. Upon exiting the culvert, flow drops ~0.5 m, preventing S12 and T12 flow from mixing.

In Subwatersheds 8 and 12, the sum of the flow at the surface and tile monitoring locations represented the total flow, whereas in Subwatershed 11, the flow at the surface monitoring location represented the total flow.

### Sample and Data Collection

Samples were collected from March to November in 2015 and 2016 using ISCO 6712 automated samplers (Teledyne ISCO) outfitted with 24 1-L bottles. The samplers were programmed to collect a 50-mL sample after a constant incremental flow volume (e.g., 100 m<sup>3</sup>) discharged through the monitoring location. Eighteen 50-mL samples, totaling 900 mL bottle<sup>-1</sup>, were deposited before the sampler moved to the next bottle. The incremental flow volume between sample collection was adjusted during site visits according to the observed flow conditions—such that the flow volume was smaller during periods of low flow and larger during periods of high flow—with the goal of collecting a minimum of two bottles per week. Samples were retrieved weekly in 2015 and every 2 wk in 2016; grab samples were also collected during each site visit. Upon retrieval from the sampler, bottles were divided into two groups: bottles containing the flow-weighted samples collected during events and those collected between events. Events were defined as any period with both a measured precipitation of >0.5 cm and an observed increase in flow. Event duration was defined as the time between when flow rate first increased and when flow rate decreased back to a steady condition. For each event, an event flow-weighted (EFW) composite sample was created by mixing all the bottles containing samples collected during the duration of the event. Likewise, baseflow flow-weighted (BFW) composite samples were created similarly. The number of bottles used to form a composite sample ranged from 1 to 24, depending on the number of bottles collected and the occurrence and duration of any events. The elapsed time for each EFW and BFW composite sample was calculated as the difference between the time the first sample in

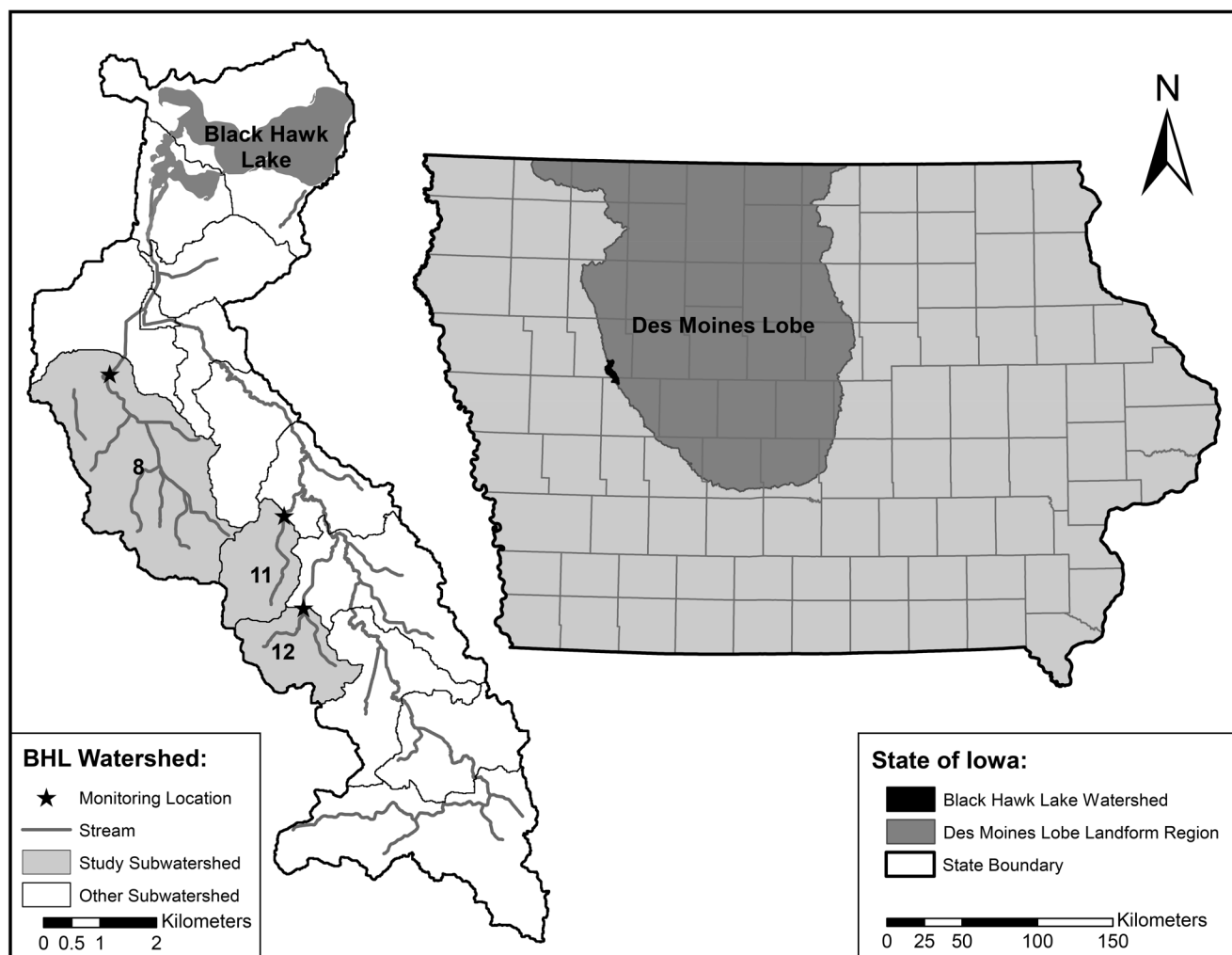


Fig. 1. Black Hawk Lake subwatersheds and monitoring locations and watershed position within the Des Moines Lobe landform region and the State of Iowa.

the first combined bottle was taken and the time the last sample in the last combined bottle was taken. Elapsed times ranged from a day up to 2 wk depending on the occurrence and duration of any events. On 12 occasions, equipment failure occurred and the automated sampler collected no flow-weighted samples. In these situations, a grab sample was substituted for the BFW composite sample. Site visits did not coincide with events; thus, no grab samples were used in place of EFW composite samples.

Water flow, velocity, and level were recorded every 5 min using ISCO 750 area velocity flow modules or ISCO 720 submerged probe flow modules. Additionally, manual measurements of velocity and depth were recorded during each site visit using a Global Water Flow Probe (Xylem). These measurements were used with known cross-sectional geometry to calculate flow rates to validate the ISCO flow module readings. Daily precipitation data were obtained using PRISM Data Explorer (PRISM, 2017).

### Sample Analysis

The BFW and EFW samples were analyzed for dissolved reactive P (DRP), TP, and TSS; the concentration data are summarized in Supplemental Fig. S4 to S6. For DRP, a 20-mL sample was filtered through a 0.45- $\mu\text{m}$  mixed cellulose membrane filter (EMD Millipore) as per Method 4500-P B.1 (APHA, 2012b),

followed by automated ascorbic acid reduction colorimetric analysis using a Seal Analytical AQ2 discrete autoanalyzer (AQ2 Method EPA-118-A Rev. 5, range = 0.01–1.0 mg P L<sup>-1</sup>, method detection limit = 0.002 mg P L<sup>-1</sup>, quantification limit = 0.02 mg P L<sup>-1</sup>). Total P was determined using a modified persulfate digestion (APHA, 2012b), followed by automated ascorbic acid reduction colorimetric analysis on a Seal Analytical AQ2 discrete autoanalyzer (AQ2 Method EPA-119-A Rev. 6, range = 0.01–1.0 mg P L<sup>-1</sup>, method detection limit = 0.003 mg P L<sup>-1</sup>, quantification limit = 0.02 mg P L<sup>-1</sup>). Samples were analyzed for TSS using Method 2540-D (method detection limit = 1 mg L<sup>-1</sup>, reporting limit = 2 mg L<sup>-1</sup>) (APHA, 2012a). Data below the detection limit were set to one half of the detection limit. The frequency of concentrations below the detection limit is summarized in Table 1.

### Data Analysis

Flow was observed throughout the entire monitoring period at both the tile and stream sites. However, negative flow measurements were erroneously recorded during low-flow conditions due to instrument sensitivity. These measurements were removed from the datasets and accounted for 0 to 10.6% of the flow data for each site. Additionally, there were several periods where the ISCO samplers failed to collect data due to loss of

power or malfunction. A summary of all data gaps is provided in Supplemental Fig. S1 and Supplemental Table S2. Overall, gaps in the flow dataset were generally under an hour. However, the maximum gap length was 18.9 d and occurred at site S11.

Water yield (WY) and the corresponding ratio of WY to precipitation, termed outflow ratio (OR), were calculated for each of the three BHL subwatersheds for both study years. Because WY and OR are dependent on total flow volume, the gaps in flow data were filled to calculate these values. Previous studies have used interpolation techniques to fill gaps in flow data (Manak and Mysak, 1989; Bourgault and Koutitonsky, 1999; Yawson et al., 2005; Schneider et al., 2007). Here, linear interpolation was used to fill gaps <5 d, and the seasonal average flow rate was used for gaps >5 d (Yawson et al., 2005). Water yields were calculated by dividing the total subwatershed outflow volume (calculated by trapezoidal integration of flow by time) by the subwatershed area. Outflow ratios were then calculated by dividing the subwatershed WY by the total subwatershed precipitation depth. There are no datasets summarizing the extent of subsurface drainage within the BHL watershed. However, Steinwand and Fenton (1995) observed lateral flow from upland well-drained soils to lower-lying poorly drained soils in the Des Moines Lobe landform region, where the BHL watershed is also located. Therefore, the entire subwatershed areas were assumed to contribute to drainage flow, because interflow occurs between areas both benefitting and not benefitting from drainage and thus would be intercepted by drain lines. Furthermore, farmers are unlikely to drain only part of a field. The implication of this assumption is that the unit-area loads calculated for the drainage pathways are conservative because the cumulative analyte loads are distributed over the entire subwatershed area.

Kendall's  $\tau$  correlation analyses were performed using JMP (SAS Institute, 2015) to identify correlations between weighted-average flow and the TP, DRP, and TSS concentrations of all EFW and BFW composite samples with corresponding flow data. Analyses were performed on the combined 2 yr of data for sites T8, S11, and S12. However, site S8 was omitted from the analysis because flow only occurred at the site during significant runoff events (seven times during the study period). Concentration data below the detection limit were set to one half of the detection limit for the analyses, and correlations were considered significant at  $p \leq 0.05$ .

Cumulative loads were calculated by multiplying analyte concentration by the weighted-average flow for each BFW or EFW

sample, then normalized by subwatershed area to produce unit-area loads. The ratio of the EFW component to the total unit-area load is referred to as the event contribution.

Annual recurrence intervals (ARIs) were calculated for events by first conducting a sliding window analysis to determine cumulative precipitation over windows ranging in length from 5 min to 7 d. Next, ARIs were calculated by performing a linear interpolation between precipitation depths from the NOAA Atlas 14 Precipitation Frequency Data Server (NOAA, 2017).

## Results

### Precipitation and Hydrology

During the study, the recorded precipitation was similar at each of the three BHL subwatersheds and ranged from 107.5 to 111.5 cm during the 2015 monitoring period and 76.7 to 78.6 cm during the 2016 monitoring period. On average, the BHL subwatersheds experienced 28.8% more precipitation in 2015 than in 2016. As evidence of this, events in 2015 had greater average depths and intensities than those in 2016 (Table 2). Water yields were calculated for each subwatershed based on the March to November sampling season of each year and ranged from 15.9 to 30.0 cm (Table 2). Overall, WYs in 2015 were similar in the three subwatersheds, but in 2016, the Subwatershed 12 WY was higher than those of Subwatersheds 8 and 11 (Table 2).

Flow patterns were also similar among the three BHL subwatersheds. The flow per area exceedance curves for each of the BHL subwatersheds (Supplemental Fig. S2) had similar shapes, indicating comparable flow responses. Constant linear trends were reflected through the majority of the curves for all three of the subwatersheds, indicating steady flow conditions. For example, the difference in the unit-area flow at 20 and 70% exceedance probabilities was  $0.0001 \text{ m}^3 \text{ s}^{-1} \text{ ha}^{-1}$ . This demonstrates that flow is sustained at a generally constant rate throughout the monitoring period, indicating a strong subsurface drainage influence (Schilling and Helmers, 2008). From 0 to 10% exceedance probabilities, the curves are steep, representing high flows over short time periods, reflective of precipitation events. Of the three subwatersheds, Subwatershed 11 experienced the most low-flow conditions (Supplemental Fig. S2).

During the study, the highest median EFW concentration for all analytes were observed at the grassed waterway site S8 (Table 1). Median EFW TP concentrations ranged from 0.034 to  $1.490 \text{ mg P L}^{-1}$  (Table 1, Supplemental Fig. S4). Median EFW and BFW

**Table 1. Analyte summary of event flow-weighted (EFW) and baseflow flow-weighted (BFW) samples for three tile-drained catchments in the Black Hawk Lake watershed.**

Site	n	Total P		Dissolved reactive P		Total suspended solids	
		Median (range)	Nondetect	Median (range)	Nondetect	Median (range)	Nondetect
		mg P L <sup>-1</sup>	%	mg P L <sup>-1</sup>	%	mg L <sup>-1</sup>	%
EFW concentrations							
Subwatershed 8 grassed waterway, S8	7	1.490 (1.277–3.848)	0.0	1.038 (0.727–1.549)	0.0	69.0 (24.0–296.0)	0.0
Subwatershed 8 tile outlet, T8	27	0.138 (0.019–4.709)	0.0	0.048 (0.001–1.177)	18.5	9.3 (0.5–496.0)	7.4
Subwatershed 11 surface, S11	14	0.164 (0.0015–3.118)	7.1	0.028 (0.001–0.203)	14.3	34.8 (1.3–2,026.0)	0.0
Subwatershed 12 surface, S12	20	0.055 (0.016–0.751)	0.0	0.006 (0.001–0.316)	30.0	20.3 (1.7–108.0)	0.0
Subwatershed 12 tile outlet, T12	19	0.034 (0.0015–0.133)	5.3	0.005 (0.001–0.067)	36.8	6.3 (0.5–37.0)	21.1
BFW concentrations							
Subwatershed 8 tile outlet, T8	46	0.04 (0.0015–0.491)	2.2	0.013 (0.001–0.191)	28.3	4.8 (0.5–119.0)	17.4
Subwatershed 11 surface, S11	47	0.032 (0.0015–1.419)	6.4	0.004 (0.001–0.475)	40.4	12.8 (0.5–852.0)	14.9
Subwatershed 12 surface, S12	50	0.055 (0.0015–1.048)	4.0	0.004 (0.001–0.125)	44.0	7.3 (0.5–244.0)	24.0
Subwatershed 12 tile outlet, T12	47	0.008 (0.0015–0.021)	34.9	0.005 (0.001–0.226)	36.2	1.3 (0.5–29.7)	44.7

**Table 2. Summary of hydrological properties for three tile-drained catchments in the Black Hawk Lake watershed for 2015 and 2016.**

Property	Subwatershed	2015	2016
No. of events		15	16
Avg. event depth (cm)		3.38	2.93
Avg. event intensity (cm h <sup>-1</sup> )		0.54	0.52
Precipitation (cm)	8	111.5	77.2
	11	107.5	76.7
	12	107.6	78.6
Water yield (cm)	8	26.2	15.9
	11	23.9	17.2
	12	27.5	30
Outflow ratio (%)	8	23	21
	11	22	22
	12	26	38

TSS concentrations were greater at the three surface sites than at the tile outlets (Table 1, Supplemental Fig. S6). The EFW DRP concentrations at the two tile outlets (Table 1, Supplemental Fig. S5) ranged from 0.001 to 1.177 mg P L<sup>-1</sup>. Soils in the region are dominated by the Clarion (fine-loamy, mixed, superactive, mesic Typic Hapludolls)–Nicollet (fine-loamy, mixed, superactive, mesic Aquic Hapludolls)–Webster (fine-loamy, mixed, superactive, mesic Typic Endoaquolls) soil association (Supplemental Table S1), which were formed in glacial till under prairie vegetation and typically have high P sorption capacity (Hoover et al., 2015). Furthermore, no surface intakes were identified in the BHL subwatersheds during a windshield survey and communications with the watershed coordinator. The lack of surface intakes eliminates a primary pathway of P to subsurface drains.

### Flow-Analyte Relationships

Overall, correlations between flow and the TP, DRP, and TSS concentrations of the BFW and EFW composite samples varied between the BHL sites. Time-series plots of precipitation, discharge, and analyte concentration are included in Supplemental Fig. S7 to S21. For the BFW samples, no significant correlations were observed between flow and analyte concentration at site T8 (Table 3). However, at site S11, a significant negative

correlation was observed between flow and BFW DRP concentration ( $p = 0.0017$ ). Significant negative correlations were also observed at site S12 between flow and BFW TSS concentration ( $p = 0.0255$ ), and at site T12 between flow and BFW TP concentration ( $p = 0.0287$ ).

In contrast, positive significant correlations between flow and EFW analyte concentrations were observed (Table 3). Significant positive correlations were observed between flow and EFW DRP concentration at sites T8 ( $p = 0.0311$ ), S11 ( $p = 0.0135$ ), and S12 ( $p = 0.0001$ ). At site S12, a significant positive correlation was also observed between flow and EFW TSS concentration ( $p = 0.0077$ ), and at site T12, a significant positive correlation was observed between flow and EFW TP concentration ( $p = 0.0141$ ).

Unit-area flow exceedance curves (Fig. 2) were developed for the daily average flow at the two tile sites (T8 and T12) and two stream sites (S11 and S12), overlaid with the BFW and EFW TP concentration data corresponding to the flow exceedance probability for the flow rate recorded when the samples were collected, and referenced to a TP value of 0.05 mg P L<sup>-1</sup>. Exceedance curves were not created for the grassed waterway (S8) because flow only occurred during significant precipitation events. Total P concentrations often exceeded the 0.05 mg P L<sup>-1</sup> threshold during all flow conditions, with concentrations frequently >10 times and up to 94 times greater than 0.05 mg P L<sup>-1</sup>. Overall, 9.8% of T12 samples, 59.7% of T8 samples, 48.3% of S11 samples, and 63.0% of S12 samples exceeded 0.05 mg P L<sup>-1</sup>.

### Analyte Loads

Due to greater precipitation, greater analyte loads were observed in 2015 than in 2016 (Fig. 3). Averaged between the three subwatersheds, loads in 2015 accounted for 78.1% of the 2-yr cumulative subwatershed TP export, 86.9% of the DRP export, and 79.5% of the TSS export. In both years, Subwatershed 11 had the greatest TP unit-area load (2.997 and 0.353 kg P ha<sup>-1</sup>), and Subwatershed 12 had the lowest DRP unit-area load (0.234 and 0.039 kg P ha<sup>-1</sup>) of the three subwatersheds. Overall, the ratio of total DRP exported to total TP exported

**Table 3. Flow-analyte correlations for baseflow flow-weighted samples (BFW) and event flow-weighted samples (EFW) for subsurface tile sites (T8 and T12) and surface water sites (S11 and S12) in the Black Hawk Lake watershed.**

Site	Analyte†	BFW				EFW			
		Kendall $\tau$	$p$ value	$n$	Samples < detection limit	Kendall $\tau$	$p$ value	$n$	Samples < detection limit
T8	DRP	0.1567	0.1422	45	13	0.2986*	0.0311	27	5
	TP	0.1067	0.3041	45	1	0.0799	0.5593	27	0
	TSS	-0.0451	0.6661	45	8	0.0172	0.9004	27	2
S11	DRP	-0.3510**	0.0017	44	18	0.5000*	0.0135	14	2
	TP	0.0269	0.8000	44	2	0.3407	0.0897	14	1
	TSS	0.1012	0.3406	44	6	0.3407	0.0897	14	0
S12	DRP	0.1376	0.2097	47	22	0.6414***	0.0001	20	6
	TP	-0.0312	0.7616	47	2	0.1170	0.4744	20	0
	TSS	-0.2837**	0.0063	47	12	0.4339**	0.0077	20	0
T12	DRP	-0.0972	0.3982	42	17	0.2937	0.0964	19	7
	TP	-0.2505*	0.0287	42	15	0.4130*	0.0141	19	1
	TSS	0.2250	0.0521	42	21	0.3303	0.0526	19	4

\* Significant at the 0.05 probability level.

\*\* Significant at the 0.01 probability level.

\*\*\* Significant at the 0.001 probability level.

† DRP, dissolved reactive P; TP, total P; TSS, total suspended solids.

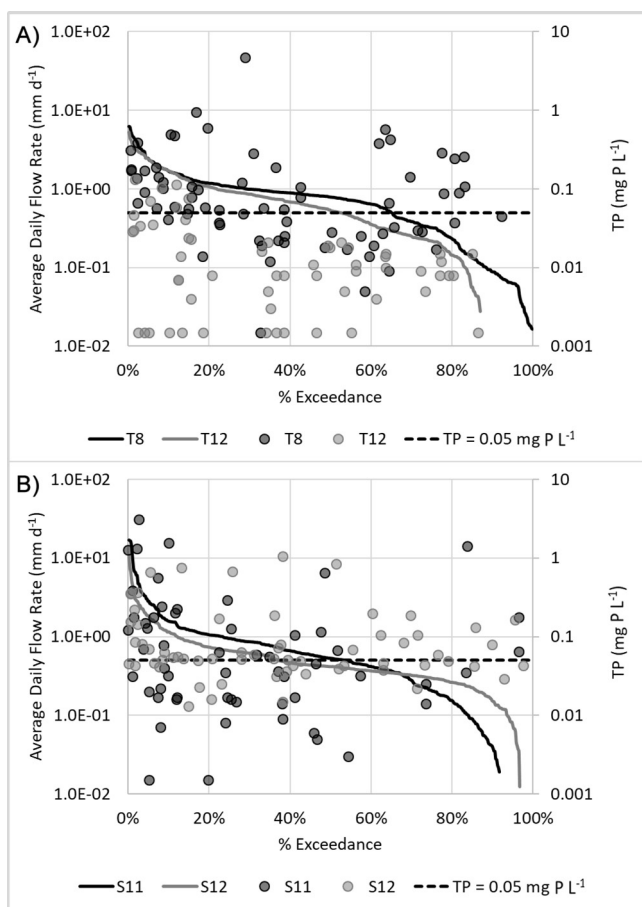


**Fig. 2.** Unit-area flow exceedance curves combined with total P (TP) concentrations for March to November 2015 and 2016 at (A) tile monitoring sites and (B) stream monitoring sites. Observed values are compared with a TP value of  $0.05 \text{ mg P L}^{-1}$  for reference.

during the 2-yr monitoring period from each subwatershed was lowest in Subwatershed 11 (0.13), followed by Subwatershed 12 (0.35) and Subwatershed 8 (0.47).

In 2015, 63.9% of the total TP export, 82.2% of the total DRP export, and 61.8% of the total TSS export from Subwatershed 11 occurred during a 9-d period between 22 June and 30 June (Supplemental Fig. S3). Precipitation during this event totaled 10.5 cm. The maximum ARI for this storm was a 3.57-yr, 3-d event. In 2016, 46.6% of the total TP export, 84.0% of the total DRP export, and 81.0% of the total TSS export from Subwatershed 11 occurred during a 6-d period between 26 April and 1 May. During this period, Subwatershed 11 received a total of 6.5 cm of precipitation. However, the storm was not large enough to interpolate an ARI (i.e.,  $\text{ARI} < 1 \text{ yr}$ ). In Subwatershed 11, crops are planted to the stream edge and there is poor stream-bank stability. Other times extreme precipitation events resulted in great TSS losses. For example, during the 22 June to 30 June 2015 event, the unit-area TSS loss from Subwatershed 11 was  $\sim 1870 \text{ kg ha}^{-1}$ .

### Surface and Drainage Partitioning

Monitoring in Subwatershed 8 allowed for separate collection of surface runoff via grassed waterway and tile pathways, which facilitate an analysis of the surface vs. drainage analyte concentrations and loads. Of the five monitoring locations, the grassed waterway (S8) had the highest median

EFW concentration for all analytes (Table 1). Despite this, the grassed waterway contributions to subwatershed loads were small because flow rarely occurred. During the 2-yr period, T8 contributed 95.1% of the total subwatershed WY, 69.8% of the cumulative subwatershed TP load, 59.2% of the DRP load, and 82.6% of the TSS load, demonstrating subsurface drainage can be a significant transport pathway. Overall, 39.8% of the Subwatershed 8 drainage TP load occurred as DRP versus 63.2% for the surface TP load.

## Discussion

### Hydrology

In the three BHL subwatersheds, WYs ranged from 15.9 to 30.0 cm and outflow ratios ranged from 21 to 38% (Table 2). Water yields for the three subwatersheds in 2015 are similar to the  $24.7 \text{ cm yr}^{-1}$  observed by Ikenberry et al. (2014) and the  $26.3 \text{ cm yr}^{-1}$  WY estimated for the entire Des Moines Lobe (IDALS, 2012). In 2016, less precipitation occurred and the WYs in Subwatersheds 8 and 11 decreased correspondingly. However, flow through the tile pathway in Subwatershed 12 was more consistent in 2016 than in 2015 and, consequently, the WY in Subwatershed 12 was higher. The BHL ORs are within the range of reported OR in undrained fields (15–27%) and drained fields and watersheds (31–88%); annual precipitation in these studies were similar to those observed in the BHL subwatersheds and ranged from 64.1 to 131.5 cm (Eastman et al., 2010; Ikenberry et al., 2014; King et al., 2015).

### Flow-Analyte Relationships

In the BHL watershed, all significant correlations between flow rate and BFW analyte concentration were negative, whereas all significant correlations between flow rate and EFW analyte concentrations were positive (Table 3). However, it is also important to note that many of the correlations did not produce statistically significant relationships. When evaluating the percentage of total analyte export that occurred at flow percentiles, a few trends emerged. For EFW samples, 69 (T8) to 93.7% (S11) of DRP export occurred during flows exceeding the 75th percentile of measured flow rates (Supplemental Table S3). Similarly, more than half of the TP load, 55.6 (T8) to 76.2% (S12), occurred during the top 25% of flows. Contrastingly, during BFW sampling,  $< 52.2\%$  (S11) of the TP load occurred during the top 25% of flows from all sites (Supplemental Table S4). When combining EFW and BFW samples,  $> 75\%$  of DRP and 66% of TP was exported during the top 25% of flows from all sites (Supplemental Table S5).

As in the BHL watershed, previous studies have also found varying relationships between concentration and flow. King et al. (2015) found that drainage TP and DRP concentrations were highest when flow exceeded the 75th percentile of measured flow rates. Likewise, Royer et al. (2006) found that an average of 84% of DRP export occurred during extreme discharges ( $\geq 90\text{th}$  percentile), which compares with an average DRP export of 78.5% for all sites reported here. These results demonstrate that overall higher loads were associated with higher flow conditions, but sample concentration was not consistently correlated with flow.

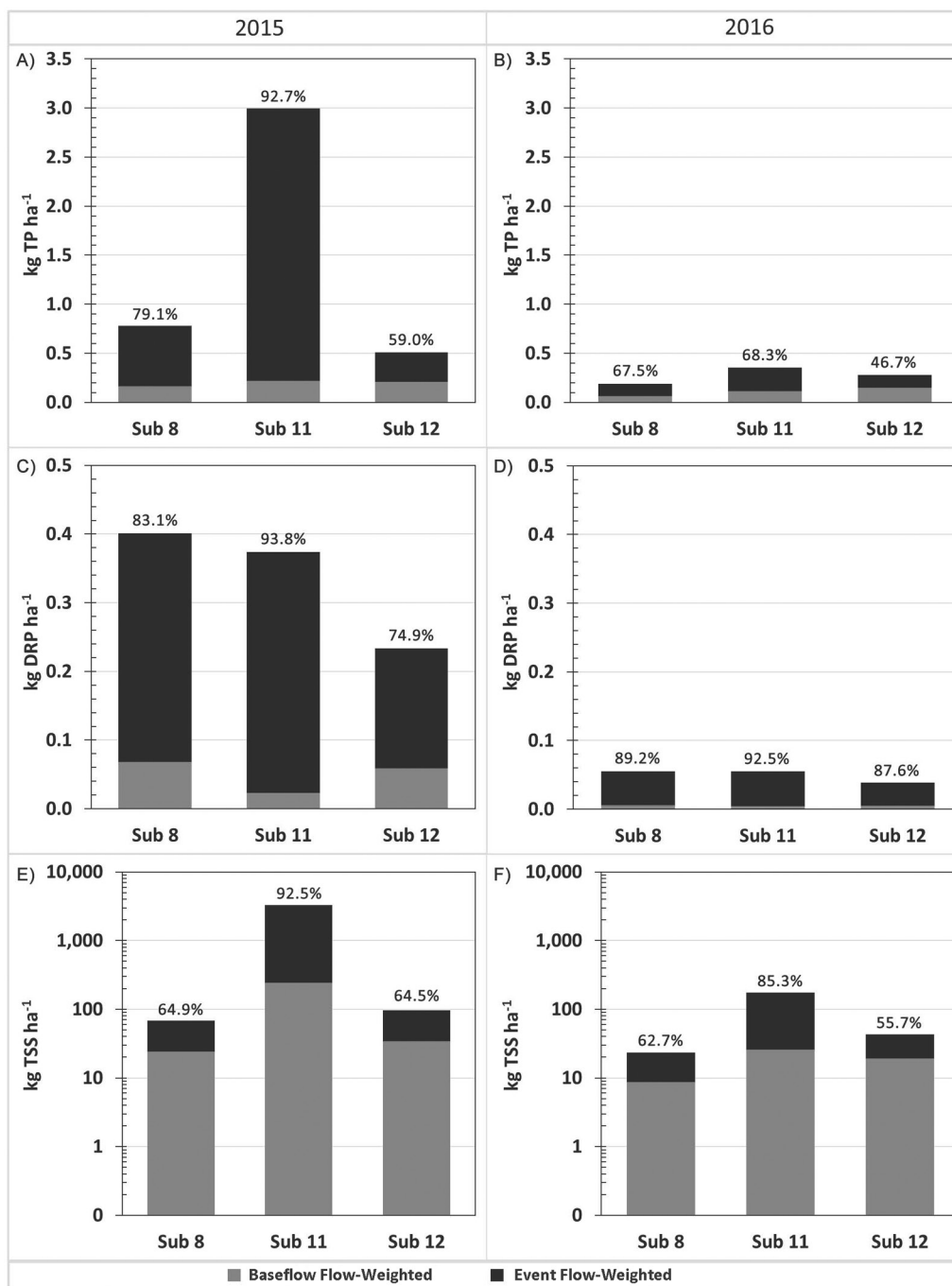


Fig. 3. Annual subwatershed unit-area loads of (A, B) total P (TP), (C, D) dissolved reactive P (DRP), and (E, F) total suspended solids (TSS). Data labels represent the percentage of the total export occurring during events.

### Dissolved Reactive Phosphorus/Total Phosphorus Ratios

Low DRP/TP ratios indicate more surface transport of particulate P (Royer et al., 2006), and higher ratios indicate greater soluble P. In the BHL watershed, the ratio of total DRP to TP exported during the 2-yr study was 0.13 in Subwatershed 11. This ratio is similar to the soluble reactive P/TP ratios of 0.15 observed in two extensively drained agricultural watersheds (3240 and 16,395 km<sup>2</sup>) in Ohio (Baker and Richards, 2002). However, BHL Subwatersheds 8 and 12 had higher DRP/TP ratios of 0.47 and 0.35, respectively. These values are within the range of unfiltered orthophosphorus/TP ratios (0.08–0.68) observed by Schilling et al. (2017) in 12 Iowa watersheds

(88–6959 km<sup>2</sup>), but lower than watersheds located in the tile-drained watersheds in the Des Moines Lobe of Iowa (>0.60).

### Impact of Event Flow and Total Loss

These results highlight the importance of precipitation events in P and TSS export. During the 2-yr study, events were responsible for 46.7 to 92.7% of annual subwatershed TP export, 74.9 to 93.8% of annual subwatershed DRP export, and 55.7 to 92.5% of annual subwatershed TSS export (Fig. 3). Sharpley et al. (2008) also observed large event contributions with 50 to 89% of TP, 45 to 78% of dissolved P, and 56 to 93% of particulate P export occurring in stormflow. In addition, Gburek and Sharpley (1998) found stormflow was responsible for ~70% of dissolved

P export. Other studies, however, have observed greater export during baseflow. A study by Novak et al. (2003) found that 57 to 71% of total dissolved P was exported during baseflow, and a report by Barr (2016) found events only contributed ~29% of the total suspended sediment load measured at two locations on the Big River in Missouri. The partitioning of export between baseflow and stormflow could differ between these studies because of differences in monitoring scale. The BHL subwatersheds range in area from 221 to 823 ha, whereas Gburek and Sharpley (1998) and Sharpley et al. (2008) both studied a 39.5-ha subwatershed, Gburek and Sharpley (1998) studied an additional 26-ha subwatershed, and Novak et al. (2003) studied a 2312-ha watershed divided into subwatersheds with areas ranging from 425 to 1036 ha. Maximum event water contributions to stormflow decrease with increasing catchment size (Brown et al., 1999).

It is well documented that a few events can account for significant portions of annual flow and contaminant loads (Novak et al., 2003; Gentry et al., 2007; Sharpley et al., 2008). Precipitation events signify the highest flow rates and P concentrations and define the source areas for the formation of surface runoff (Gburek and Sharpley, 1998). In BHL Subwatershed 11, precipitation over a 9-d event (maximum ARI = 3.57 yr, 3 d) was responsible for 63.9, 82.2, and 61.8% of the total 2015 subwatershed export of TP, DRP, and TSS, respectively. In 2016, 46.6, 84.0, and 81.0% of the respective total annual export of TP, DRP, and TSS from Subwatershed 11 occurred during a 6-d event (ARI < 1 yr). These two events likely represent worst-case scenarios for suspended solids losses and associated P losses. Prolonged periods of precipitation overwhelm soil infiltration capacity, leading to surface runoff. Overall, results from Subwatershed 11 indicate that even frequent small precipitation storms (ARI < 1 yr) have the potential to result in extreme P and TSS losses. Therefore, designing BMPs that reduce P losses during these small events could provide significant reductions in P losses while minimizing cost. A similar conclusion was reached by Sharpley et al. (2008) that found the largest storms (ARI > 10 yr) were responsible for only 20% of P exported during a 10-yr study.

## Surface and Drainage Partitioning

Of the five BHL monitoring locations, the grassed waterway had the highest median EFW concentration for all analytes (Table 1). Flow only occurred in the grassed waterway over short periods during extreme precipitation events. Therefore, median analyte concentrations could be highest at the grassed waterway because flow-weighted samples were only able to be collected during the short periods of peak flow conditions, whereas samples were collected for the entire hydrograph at the other four sites. However, grassed waterways are typically ineffective at removing dissolved nutrients even though they have been shown to control erosion (Shipitalo and Edwards, 1996). Fiener and Auerswald (2009) measured runoff DRP concentrations from watersheds with and without hydrodynamically rough grassed waterways implemented. They concluded that grassed waterways had little impact on DRP concentration, and the related DRP load reduction simply corresponded to the decrease in total runoff.

Although the grassed waterway had the highest median EFW concentrations for all analytes, the fraction of the total analyte

export from Subwatershed 8 via the grassed waterway was small because of the dominance of the drainage pathway. Over the 2-yr period, the tile outlet was responsible for 69.8% of the cumulative subwatershed TP load, 59.2% of the DRP load, and 82.6% of the TSS load. Others have also observed substantial drainage TP contributions through drainage, ranging from 17 to >50% of the total P losses (Culley et al., 1983; Jamieson et al., 2003; Tomer et al., 2010; Enright and Madramootoo, 2004; King et al., 2015; Smith et al., 2015). However, several field-scale studies have concluded that subsurface drainage could reduce overall P export by reducing surface runoff (Bottcher et al., 1981; Bengtson et al., 1988; Fausey et al., 1995; Eastman et al., 2010). This suggests that field-scale P transport pathways may be highly sensitive to field conditions and properties and may not reflect overall P transport at the catchment scale.

Phosphorus losses in the drainage pathway in Subwatershed 8 were primarily particulate associated, which was unexpected given the presence of drainage and the grass waterway. Overall, only 39.8% of Subwatershed 8 drainage TP load occurred as DRP. Although particulate P has been reported to be the major fraction of TP in drainage water in some cases (Uusitalo et al., 2001; Vidon and Cuadra, 2011), P losses in drainage are typically dominated by the dissolved form (Heckrath et al., 1995; Gächter et al., 1998; Haygarth et al., 1998; Kinley et al., 2007). The unexpected results in the BHL subwatershed could potentially be explained by macropore flow conditions in no-till managed areas or the presence of surface intakes (although windshield survey and communication with the watershed coordinator did not indicate their presence). Another possible explanation is that the particulate matter in the drainage flow is P enriched; McDowell et al. (2004) found that particulate P enrichment ratios increased with decreasing erosion. Thus, subsurface drainage could be reducing surface runoff and erosion, leading to greater P enrichment of the particulate matter, which is then exported via the drainage pathway.

## Conclusions

Results from the BHL watershed show that analyte concentrations were positively correlated with flow during events, but not during baseflow conditions. Single events accounted for an overwhelming majority of annual losses in Subwatershed 11; two events were responsible for up to 63.9, 84.0, and 81.0% of annual subwatershed exports of TP, DRP, and TSS, respectively. These results show that even frequent, low-depth storms have the potential to cause extreme P and TSS losses. These findings highlight the importance of single events and show how site-specific conditions influence P and TSS losses. Focusing BMP design to reduce P losses during frequent small events therefore has the potential to significantly reduce P export while minimizing construction costs. A comparison between surface and drainage transport pathways demonstrated that TP, DRP, and TSS losses through drainage are significant and that the presence of drainage did not decrease overall TP export, and thus conservation practices designed to treat P in drainage are needed. Finally, these results provide evidence that particulate P losses in drainage waters can be greater than dissolved P losses. Understanding these relationships is important for remediation strategies and to assist in targeting areas for BMP implementation.

## Supplemental Material

Details about subwatershed properties, flow exceedance curves, gaps in flow data, cumulative loads, time series data, and sampling results are included as supplemental material.

## Acknowledgments

Funding for this project was provided by Iowa Department of Natural Resources contract 14ESDWQBCIKEN-0001, USEPA Section 319, and the Iowa Water Center. The authors would like to thank T.J. Lynn, the watershed coordinator for the Black Hawk Lake Watershed Project; Carl Pederson for assistance with field instrumentation; and Katherine van der Woude for assistance with sample collection and analysis.

## References

- Alexander, R.B., R.A. Smith, G.E. Schwarz, E.W. Boyer, J.V. Nolan, and J.W. Brakebill. 2008. Differences in phosphorus and nitrogen delivery to the Gulf of Mexico from the Mississippi River basin. *Environ. Sci. Technol.* 42:822–830. doi:10.1021/es0716103
- Algoazany, A., P. Kalita, G. Czapar, and J. Mitchell. 2007. Phosphorus transport through subsurface drainage and surface runoff from a flat watershed in east central Illinois, USA. *J. Environ. Qual.* 36:681–693. doi:10.2134/jeq2006.0161
- APHA. 2012a. Part 2000 physical & aggregate properties: 2540 D. Total suspended solids dried at 103–105°C. In: E. W. Rice, et al., editors, *Standard methods for the examination of water and wastewater*. 22nd ed. Am. Public Health Assoc., Washington, DC. p. 2-58–2-59.
- APHA. 2012b. Part 4000 inorganic nonmetallic constituents: 4500-P B. sample preparation. In: E.W. Rice, et al., editors, *Standard methods for the examination of water and wastewater*. 22nd ed. Am. Public Health Assoc., Washington, DC. p. 4-149–4-151.
- Baker, D.B., and R.P. Richards. 2002. Phosphorus budgets and riverine phosphorus export in northwestern Ohio watersheds. *J. Environ. Qual.* 31:96–108. doi:10.2134/jeq2002.9600
- Barr, M.N. 2016. Surface-water quality and suspended-sediment quantity and quality within the Big River basin, southeastern Missouri, 2011–13. *Sci. Invest. Rep.* 2015-5171. USGS, Reston, VA. doi:10.3133/sir20155171
- Behrendt, H., and A. Bachor. 1998. Point and diffuse load of nutrients to the Baltic Sea by river basins of North East Germany (Mecklenburg-Vorpommern). *Water Sci. Technol.* 38:147–155. doi:10.2166/wst.1998.0396
- Bengtson, R., C. Carter, H. Morris, and S. Bartkiewicz. 1988. The influence of subsurface drainage practices on nitrogen and phosphorus losses in a warm, humid climate. *Trans. ASAE* 31:0729–0733. doi:10.13031/2013.30775
- Blann, K.L., J.L. Anderson, G.R. Sands, and B. Vondracek. 2009. Effects of agricultural drainage on aquatic ecosystems: A review. *Crit. Rev. Environ. Sci. Technol.* 39:909–1001. doi:10.1080/10643380801977966
- Botcher, A., E. Monke, and L. Huggins. 1981. Nutrient and sediment loadings from a subsurface drainage system. *Trans. ASAE* 24:1221–1226. doi:10.13031/2013.34423
- Bourgault, D., and V.G. Koutitonsky. 1999. Real-time monitoring of the freshwater discharge at the head of the St. Lawrence Estuary. *Atmos.-ocean* 37:203–220. doi:10.1080/07055900.1999.9649626
- Brown, V.A., J.J. McDonnell, D.A. Burns, and C. Kendall. 1999. The role of event water, a rapid shallow flow component, and catchment size in summer stormflow. *J. Hydrol.* 217:171–190. doi:10.1016/S0022-1694(98)00247-9
- Culley, J., E. Bolton, and V. Berynyk. 1983. Suspended solids and phosphorus loads from a clay soil: I. Plot studies. *J. Environ. Qual.* 12:493–498. doi:10.2134/jeq1983.00472425001200040011x
- Du, B., J.G. Arnold, A. Saleh, and D.B. Jaynes. 2005. Development and application of SWAT to landscapes with tiles and potholes. *Trans. ASAE* 48:1121–1133. doi:10.13031/2013.18522
- Eastman, M., A. Gollamudi, N. Stämpfli, C. Madramootoo, and A. Sarangi. 2010. Comparative evaluation of phosphorus losses from subsurface and naturally drained agricultural fields in the Pike River watershed of Quebec, Canada. *Agric. Water Manage.* 97:596–604. doi:10.1016/j.agwat.2009.11.010
- Enright, P., and C. Madramootoo. 2004. Phosphorus losses in surface runoff and subsurface drainage waters on two agricultural fields in Quebec. In: R. Cooke, editor, *Drainage VIII—Proceedings of the 8th International Drainage Symposium*, Sacramento, CA. 21–24 Mar. 2004. ASAE, St. Joseph, MI. p. 160–170.
- Fausey, N.R., L.C. Brown, H.W. Belcher, and R.S. Kanwar. 1995. Drainage and water quality in Great Lakes and Cornbelt states. *J. Irrig. Drain. Eng.* 121:283–288. doi:10.1061/(ASCE)0733-9437(1995)121:4(283)
- Fausey, N.R., E.J. Doering, and M.L. Palmer. 1987. Purposes and benefits of drainage. In: G. Pavelis, editors, *Farm drainage in the United States: History, status, and prospects*. Misc. Publ. 1455. USDA Econ. Res. Serv., Washington, DC. p. 48–51.
- Fiener, P., and K. Auerswald. 2009. Effects of hydrodynamically rough grassed waterways on dissolved reactive phosphorus loads coming from agricultural watersheds. *J. Environ. Qual.* 38:548–559. doi:10.2134/jeq2007.0525
- Gächter, R., J.M. Ngatiah, and C. Stamm. 1998. Transport of phosphate from soil to surface waters by preferential flow. *Environ. Sci. Technol.* 32:1865–1869. doi:10.1021/es9707825
- Gburek, W.J., and A.N. Sharpley. 1998. Hydrologic controls on phosphorus loss from upland agricultural watersheds. *J. Environ. Qual.* 27:267–277. doi:10.2134/jeq1998.00472425002700020005x
- Gentry, L., M. David, T. Royer, C. Mitchell, and K. Starks. 2007. Phosphorus transport pathways to streams in tile-drained agricultural watersheds. *J. Environ. Qual.* 36:408–415. doi:10.2134/jeq2006.0098
- Geohring, L.D., O.V. McHugh, M.T. Walter, T.S. Steenhuis, M.S. Akhtar, and M.F. Walter. 2001. Phosphorus transport into subsurface drains by macropores after manure applications: Implications for best manure management practices. *Soil Sci.* 166:896–909. doi:10.1097/00010694-200112000-00004
- Haygarth, P., L. Hepworth, and S. Jarvis. 1998. Forms of phosphorus transfer in hydrological pathways from soil under grazed grassland. *Eur. J. Soil Sci.* 49:65–72. doi:10.1046/j.1365-2389.1998.00131.x
- Heathwaite, A., and R. Dils. 2000. Characterising phosphorus loss in surface and subsurface hydrological pathways. *Sci. Total Environ.* 251–252:523–538. doi:10.1016/S0048-9697(00)00393-4
- Heckrath, G., P. Brookes, P. Poulton, and K. Goulding. 1995. Phosphorus leaching from soils containing different phosphorus concentrations in the Broadbalk experiment. *J. Environ. Qual.* 24:904–910. doi:10.2134/jeq1995.00472425002400050018x
- Hoover, N.L., R. Kanwar, M.L. Soupir, and C. Pederson. 2015. Effects of poultry manure application on phosphorus in soil and tile drain water under a corn-soybean rotation. *Water Air Soil Pollut.* 226:138. doi:10.1007/s11270-015-2403-9
- Howarth, R., and H.W. Paerl. 2008. Coastal marine eutrophication: Control of both nitrogen and phosphorus is necessary. *Proc. Natl. Acad. Sci. U. S. A.* 105:E103. doi:10.1073/pnas.0807266106
- IDALS. 2012. Iowa nutrient reduction strategy: A science and technology-based framework to assess and reduce nutrients to Iowa waters and the Gulf of Mexico. Iowa Dep. Agric. Land Stewardship, Des Moines.
- Ikenberry, C.D., M.L. Soupir, K.E. Schilling, C.S. Jones, and A. Seeman. 2014. Nitrate-nitrogen export: Magnitude and patterns from drainage districts to downstream river basins. *J. Environ. Qual.* 43:2024–2033. doi:10.2134/jeq2014.05.0242
- Jamieson, A., C. Madramootoo and P. Enright. 2003. Phosphorus losses in surface and subsurface runoff from a snowmelt event on an agricultural field in Quebec. *Can. Biosyst. Eng.* 45:1-1.
- Kepler, J. and J. Rhoderick. 2015. Progressive management practices for drainage systems on the eastern shore of Maryland. Conservation Innovation Grant final report. Grant #69-3A75-11-28. USDA, Natl. Resour. Conserv. Serv., Annapolis, MD. [https://www.nrcs.usda.gov/wps/PA\\_NRC-SCONSUMPTION/download/?cid...pdf](https://www.nrcs.usda.gov/wps/PA_NRC-SCONSUMPTION/download/?cid...pdf) (accessed 7 July 2018).
- King, K.W., M.R. Williams, and N.R. Fausey. 2015. Contributions of systematic tile drainage to watershed-scale phosphorus transport. *J. Environ. Qual.* 44:486–494. doi:10.2134/jeq2014.04.0149
- Kinley, R.D., R.J. Gordon, G.W. Stratton, G.T. Patterson, and J. Hoyle. 2007. Phosphorus losses through agricultural tile drainage in Nova Scotia, Canada. *J. Environ. Qual.* 36:469–477. doi:10.2134/jeq2006.0138
- Kleinman, P.J.A., A.L. Allen, B.A. Needelman, A.N. Sharpley, P.A. Vadas, L.S. Saporito, et al. 2007. Dynamics of phosphorus transfers from heavily manured Coastal Plain soils to drainage ditches. *J. Soil Water Conserv.* 62:225–235.
- Kleinman, P.J.A., A.N. Sharpley, R.W. McDowell, D.N. Flaten, A.R. Buda, L. Tao, et al. 2011. Managing agricultural phosphorus for water quality protection: Principles for progress. *Plant Soil* 349:169–182. doi:10.1007/s11104-011-0832-9
- Kronvang, B., G.H. Rubæk, and G. Heckrath. 2009. International phosphorus workshop: Diffuse phosphorus loss to surface water bodies—Risk assessment, mitigation options, and ecological effects in river basins. *J. Environ. Qual.* 38:1924–1929. doi:10.2134/jeq2009.0051
- Manak, D.K., and L.A. Mysak. 1989. On the relationship between arctic sea-ice anomalies and fluctuations in Northern Canadian air temperature and river discharge. *Atmos.-ocean* 27:682–691. doi:10.1080/07055900.1989.9649361
- McDowell, R., B. Biggs, A. Sharpley, and L. Nguyen. 2004. Connecting phosphorus loss from agricultural landscapes to surface water quality. *Chem. Ecol.* 20:1–40. doi:10.1080/02757540310001626092

- NOAA. 2017. Precipitation Frequency Data Server (PFDS). NOAA. <https://hdsc.nws.noaa.gov/hdsc/pfds/> (accessed 21 Feb. 2018).
- Novak, J., K. Stone, D. Watts, and M. Johnson. 2003. Dissolved phosphorus transport during storm and base flow conditions from an agriculturally intensive southeastern coastal plain watershed. *Trans. ASAE* 46:1355–1363. doi:10.13031/2013.15446
- Paerl, H.W. 2009. Controlling eutrophication along the freshwater–marine continuum: Dual nutrient (N and P) reductions are essential. *Estuaries Coasts* 32:593–601. doi:10.1007/s12237-009-9158-8
- PRISM. 2017. PRISM gridded climate data. PRISM Clim. Group, Oregon State Univ. <http://prism.oregonstate.edu/> (accessed 21 Feb. 2018).
- Reeve, R.C., and N.R. Fausey. 1974. Drainage and timeliness of farming operations. In: J. van Schilfgaarde, editor, *Drainage for agriculture*. Agron. Monogr. 17. ASA, Madison, WI, p. 55–66.
- Royer, T.V., M.B. David, and L.E. Gentry. 2006. Timing of riverine export of nitrate and phosphorus from agricultural watersheds in Illinois: Implications for reducing nutrient loading to the Mississippi River. *Environ. Sci. Technol.* 40:4126–4131. doi:10.1021/es052573n
- SAS Institute. 2015. JMP Pro 14. SAS Inst., Cary, NC.
- Schilling, K.E., and M. Helmers. 2008. Effects of subsurface drainage tiles on streamflow in Iowa agricultural watersheds: Exploratory hydrograph analysis. *Hydrol. Processes* 22:4497–4506. doi:10.1002/hyp.7052
- Schilling, K.E., S.-W. Kim, C.S. Jones, and C.F. Wolter. 2017. Orthophosphorus contributions to total phosphorus concentrations and loads in agricultural watersheds. *J. Environ. Qual.* 46:828–835. doi:10.2134/jeq2017.01.0015
- Schneider, M.K., F. Brunner, J.M. Hollis, and C. Stamm. 2007. Towards a hydrological classification of European soils: Preliminary test of its predictive power for the base flow index using river discharge data. *Hydrol. Earth Syst. Sci. Discuss.* 11:1501–1513. doi:10.5194/hess-11-1501-2007
- Sharpley, A.N., P.J.A. Kleinman, A.L. Heathwaite, W.J. Gburek, G.J. Folmar, and J.P. Schmidt. 2008. Phosphorus loss from an agricultural watershed as a function of storm size. *J. Environ. Qual.* 37:362–368. doi:10.2134/jeq2007.0366
- Sharpley, A., and X. Wang. 2014. Managing agricultural phosphorus for water quality: Lessons from the USA and China. *J. Environ. Sci. (China)* 26:1770–1782. doi:10.1016/j.jes.2014.06.024
- Shipitalo, M., and W. Edwards. 1996. Effects of initial water content on macropore/matrix flow and transport of surface-applied chemicals. *J. Environ. Qual.* 25:662–670. doi:10.2134/jeq1996.00472425002500040005x
- Simard, R., S. Beauchemin, and P. Haygarth. 2000. Potential for preferential pathways of phosphorus transport. *J. Environ. Qual.* 29:97–105. doi:10.2134/jeq2000.00472425002900010012x
- Smith, D.R., K.W. King, L. Johnson, W. Francesconi, P. Richards, D. Baker, et al. 2015. Surface runoff and tile drainage transport of phosphorus in the Midwestern United States. *J. Environ. Qual.* 44:495–502. doi:10.2134/jeq2014.04.0176
- Steinwand, A., and T. Fenton. 1995. Landscape evolution and shallow groundwater hydrology of a till landscape in central Iowa. *Soil Sci. Soc. Am. J.* 59:1370–1377. doi:10.2136/sssaj1995.03615995005900050025x
- Stuart, V., D. Harker, and R. Clearwater. 2010. Watershed evaluation of beneficial management practices (WEBs): Towards enhanced agricultural landscape planning four-year review (2004/5–2007/8). *Agric. Agri-Food Canada, Ottawa, ON.*
- Tan, C., and T. Zhang. 2011. Surface runoff and sub-surface drainage phosphorus losses under regular free drainage and controlled drainage with sub-irrigation systems in southern Ontario. *Can. J. Soil Sci.* 91:349–359. doi:10.4141/cjss09086
- Tomer, M., C. Wilson, T. Moorman, K. Cole, D. Heer, and T. Isenhardt. 2010. Source-pathway separation of multiple contaminants during a rainfall-runoff event in an artificially drained agricultural watershed. *J. Environ. Qual.* 39:882–895. doi:10.2134/jeq2009.0289
- Torrent, J., E. Barberis, and F. Gil-Sotres. 2007. Agriculture as a source of phosphorus for eutrophication in southern Europe. *Soil Use Manage.* 23:25–35. doi:10.1111/j.1475-2743.2007.00122.x
- Turner, R.E., N.N. Rabalais, D. Scavia and G.F. McIsaac. 2007. Corn Belt landscapes and hypoxia of the Gulf of Mexico. In: J.I. Nassauer, et al., editors, *From the Corn Belt to the Gulf: Societal and environmental implications of alternative agricultural futures*. Resour. Future Press, Washington, DC, p. 10–27.
- Uusitalo, R., E. Turtola, T. Kauppila, and T. Lilja. 2001. Particulate phosphorus and sediment in surface runoff and drainflow from clayey soils. *J. Environ. Qual.* 30:589–595. doi:10.2134/jeq2001.302589x
- Vadas, P.A., M.S. Srinivasan, P.J.A. Kleinman, J.P. Schmidt, and A.L. Allen. 2007. Hydrology and groundwater nutrient concentrations in a ditch-drained agroecosystem. *J. Soil Water Conserv.* 62:178–188.
- Vidon, P., and P. Cuadra. 2011. Phosphorus dynamics in tile-drain flow during storms in the US Midwest. *Agric. Water Manage.* 98:532–540. doi:10.1016/j.agwat.2010.09.010
- Vos, J. 1987. Proceedings, symposium 25th International course on land drainage: Twenty-five years of drainage experience, Wageningen, the Netherlands. 24–28 Nov. 1986. *Int. Inst. Land Reclam. Improv., Int. Agric. Ctr., Wageningen.*
- Williams, M.R., K.W. King, W. Ford, A.R. Buda, and C.D. Kennedy. 2016. Effect of tillage on macropore flow and phosphorus transport to tile drains. *Water Resour. Res.* 52:2868–2882. doi:10.1002/2015WR017650
- Yawson, D., V. Kongo, and R. Kachroo. 2005. Application of linear and nonlinear techniques in river flow forecasting in the Kilombero River basin, Tanzania. *Hydrol. Sci. J.* 50:796–809. doi:10.1623/hysj.2005.50.5.783
- Zucker, L.A., and L.C. Brown. 1998. Agricultural drainage: Water quality impacts and subsurface drainage studies in the Midwest. *Ext. Bull.* 871. The Ohio State Univ., Columbus, OH.